A Directional Coupler of a Vertically Installed Planar Circuit Structure

YOSHIHIRO KONISHI, FELLOW, IEEE, IKUO AWAI, MEMBER, IEEE, YOSHIRO FUKUOKA, MEMBER, IEEE, AND MASAMITSU NAKAJIMA, MEMBER, IEEE

Abstract—**A new type of directional coupler is fabricated installing a second printed circuit board on a main board. Experimental results agree well with a numerical calculation based on the boundary element method. Compact and low-cost couplers can be created with a wide range of design parameters.**

I. Introduction

IN DESIGNING hybrid integrated circuits in UHF or microwave frequencies, it is sometimes necessary to fabricate 3-dB couplers in limited space. A conventional narrow-side coupler which consists of two parallel microstrip lines can be used for such purpose. However, its inherent weak coupling nature makes the gap between the two strips so narrow that a precise control of the gap spacing is required. An easier way of realizing a 3-dB coupler on stripline circuit is to use a hybrid ring, which requires much more space on the circuit board. Several stripline configurations have been proposed to overcome this difficulty [1]–[3].

In this paper, we propose a new design of involving a simple, practical structure for realizing a 3-dB coupler on a printed circuit board. A VIP (vertically installed planar) circuit consists basically of broadside coupled lines vertically installed on a main microstrip line circuit [4]. A typical directional coupler using a VIP circuit is shown in Fig. 1. Through conventional narrow-side coupling, it is not easy to have strong coupling between two adjacent microstrip lines. On the other hand, in the VIP configuration, the vertical substrate contributes to a strong coupling.

The newly added vertical substrate significantly increases the freedom of design parameters. Coupling parameters can be easily controlled by changing either the dielectric constants or the thicknesses of the substrates. This makes almost any coupling constant available along with good isolation and a suitable input impedance. Besides, the three-dimensional structure makes good use of the space, resulting in a compact circuit structure. In fact, the occupied area of a VIP 3-dB coupler is as small as a Lange 3-dB coupler and more than five times smaller than a hybrid ring. Employing a high-Q substrate only for the vertical part of the VIP circuit, one can easily realize a low-loss 3-dB coupler. It does not increase the material cost very much since one can still use inexpensive material for the main substrate such as glass epoxy. This feature is especially important when it is used in the mass production of consumer items.

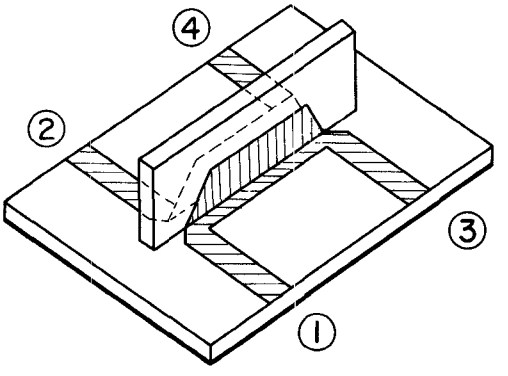

Fig. 1. Structure of a VIP directional coupler.

We will compute the characteristic impedances for even and odd modes of VIP coupled lines making use of the boundary element method (BEM) [5], and these values will be substituted into the general formulas for the response of symmetric coupled lines to give the VIP directional coupler characteristics.

Comparison of the theoretical and experimental results will show good agreement together with a relaxed tolerance in fabrication.

II. Effective Dielectric Constants and Characteristic Impedances for Even and Odd Modes in VIP Coupled Lines

It is postulated that the propagation is in quasi-TEM mode, so that the capacitance between the signal line and the ground plate is the essential quantity. The effective dielectric constant and the characteristic impedance are computed as

$$\epsilon_e = C/C_0 \tag{1}$$

$$Z_0 = \frac{1}{\sqrt{\epsilon_e} cC_0} \tag{2}$$

where c is the light velocity in free space, and C and C_0 are the capacitances between the two conductors of unit length along the transmission line with and without the dielectric materials, respectively.

Manuscript received September 25, 1987; revised January 14, 1988.

Y. Konishi, I. Awai, and Y. Fukuoka are with the Uniden Corporation, 4-7-4 Onitaka, Ichikawa, Chiba Prefecture 272, Japan.

M. Nakajima is with the Electronics Department, Kyoto University, Yoshida-honmachi, Kyoto 606, Japan.

IEEE Log Number 8821068.

0018-9480/88/0600-1057$01.00 ©1988 IEEE

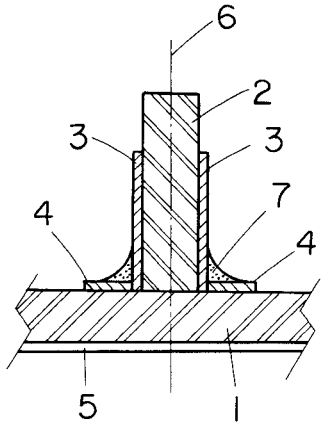

Fig. 2. Cross-sectional view of a VIP coupler. *1*–first dielectric substrate (ϵ_{r1}); *2*–second dielectric substrate (ϵ_{r2}); *3*–coupled distribution line on second dielectric substrate; *4*–distributed line connected to coupled distributed line; *5*–ground plate; *6*–symmetry plane; *7*–soldering.

Now we will proceed to obtain the capacitances C and C_0, adopting the BEM. We divide the boundaries into small elements; that is, we use the Gauss–Green formula governing the field and its derivative on the boundary:

$$\frac{1}{2}\phi = \int_\Gamma \frac{\partial \phi}{\partial n} \cdot \phi^* \, d\Gamma - \int_\Gamma \phi \cdot \frac{\partial \phi^*}{\partial n} \, d\Gamma. \tag{3}$$

This formula is discretized into

$$\frac{1}{2}\phi_i = \sum_{j=1}^{m} \left\{ \frac{\partial \phi_j}{\partial n} \int_{\Gamma_j} \phi^* \, d\Gamma - \phi_j \int_{\Gamma_j} \frac{\partial \phi^*}{\partial n} \, d\Gamma \right\}. \tag{4}$$

This is a set of m simultaneous linear equations for m unknowns, where

- ϕ potential at the boundaries,
- $\frac{\partial \phi}{\partial n}$ normal derivative of potential at the boundaries,
- Γ boundaries including the electric or magnetic walls and the borders of two adjacent materials,
- ϕ^* two-dimentional Green's function: $-\frac{1}{2\pi\epsilon} \ln r$,
- r distance between ith and jth elements,
- i, j serial numbers of the boundary elements.

On electrodes (electric walls) the ϕ_i's are known while the $\partial\phi_i/\partial n$'s are unknown. On magnetic walls, however, the $\partial\phi_i/\partial n$'s are known (zero) while the ϕ_i's are unknown. Across the boundaries of different materials, ϕ_i and $\partial\phi_i/\partial n$ should be continuous. The number of unknown variables and equations should coincide, so that we can solve the simultaneous equations numerically with the aid of a computer.

The quantities $\partial\phi/\partial n$ on the electrode calculated above are integrated to obtain the total charge on the electrode and consequently the capacitances C and C_0 between the electrode and the ground plate. One can find the characteristic impedance and effective permittivity by substituting these capacitances into (1) and (2).

The cross-sectional view of the VIP coupled lines is shown in Fig. 2. Noting that it has a symmetric structure, the electric field distribution for even and odd excitation is roughly depicted in Fig. 3. In the BEM calculation, the vertical line of symmetry is taken as magnetic and electric walls for even and odd mode, respectively. When we create a directional coupler it is important to have equal propagation constants, i.e., equal effective dielectric constants, ϵ_{ee} and ϵ_{eo}, for even and odd mode. Otherwise, we will have a poor return loss and directivity in the passband. In order to satisfy this condition, it is necessary to keep $\epsilon_{r1} > \epsilon_{r2}$, because more electric flux passes through free space in the even mode excitation (see Fig. 3).

We have shown in Fig. 4 a basic set of parameters with typical numerical values. Calculation was carried out using

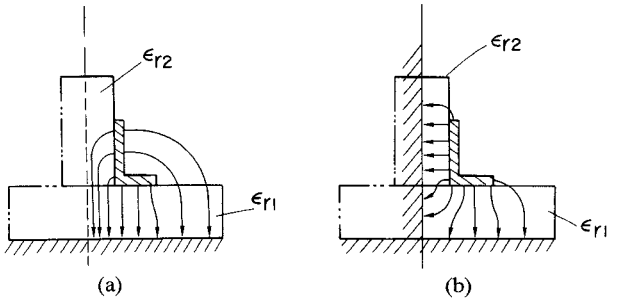

Fig. 3. Electric field distribution for (a) even and (b) odd modes.

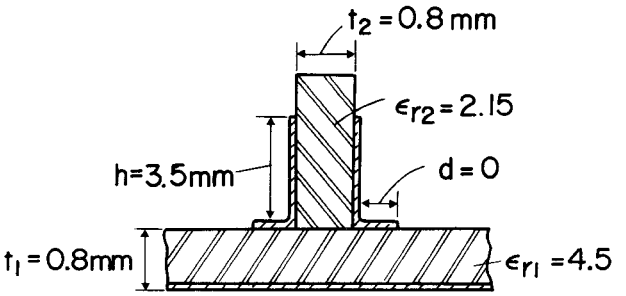

Fig 4. A set of parameters for numerical calculation.

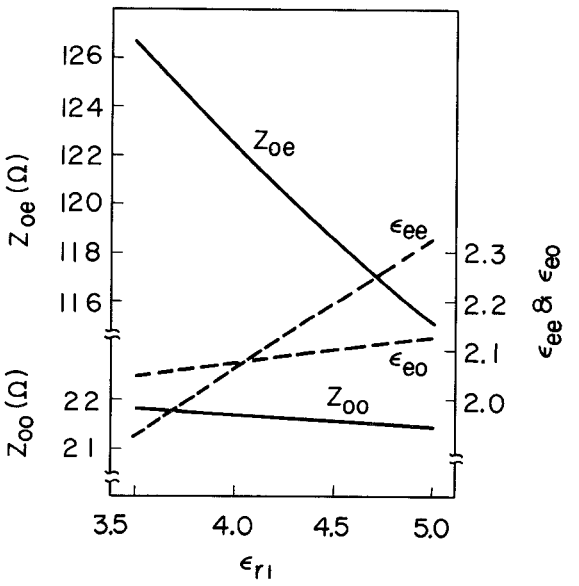

Fig. 5. Effective permittivities and characteristic impedances versus permittivity of main substrate ($t_1 = 0.8$ mm, $\epsilon_{r2} = 2.15$, $t_2 = 0.8$ mm, $h = 3.5$ mm, $d = 0$).

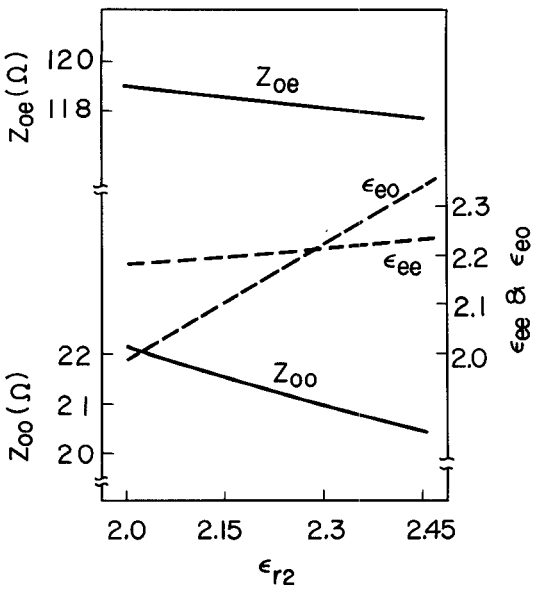

Fig. 6. Effective permittivities and characteristic impedances versus permittivity of vertical substrate ($\epsilon_{r1} = 4.5$, $t_1 = 0.8$ mm, $t_2 = 0.8$ mm, $h = 3.5$ mm, $d = 0$).

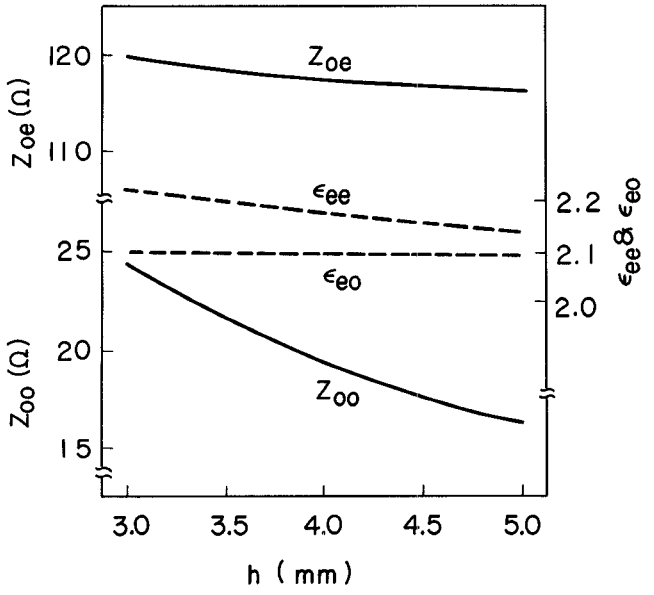

Fig. 7. Effective permittivities and characteristic impedances versus electrode height on vertical substrate ($\epsilon_{r1} = 4.5$, $t_1 = 0.8$ mm, $\epsilon_{r2} = 2.15$, $t_2 = 0.8$ mm, $d = 0$).

the values in Fig. 4 unless otherwise specified in each figure. Examination of the calculated results in Figs. 5 and 6 notifies us that the permittivity of the vertical substrate determines Z_{0o} while that of the main substrate gives Z_{0e}. This property is well understood referring to Fig. 3(a) and (b): the electric flux is strongly confined in the vertical substrate for the odd mode and in the main substrate for the even mode.

Fig. 7 indicates the same tendency as Fig. 6; that is, the variation of the electrode height on the vertical substrate mainly affects the odd mode. The thickness of VIP substrate, on the other hand, exerts influence on both modes (Fig. 8). It is physically understood from Fig. 3 that the odd-mode impedance decreases with thinner vertical substrate, while the even-mode impedance increases at the same time.

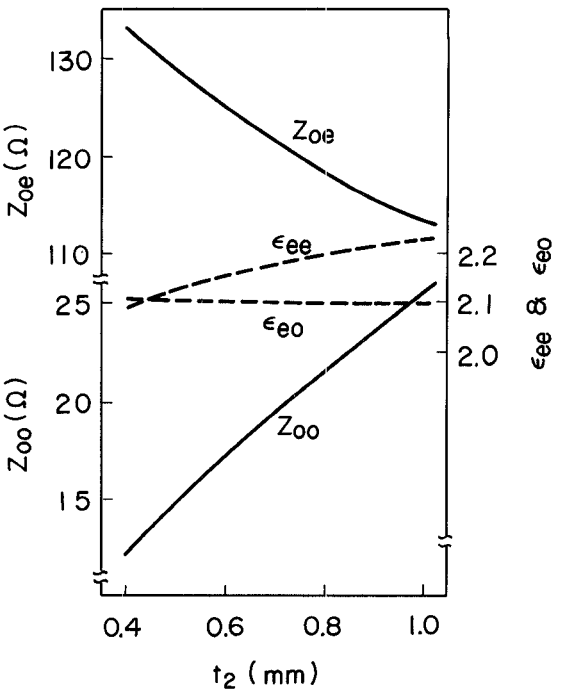

Fig. 8. Effective permittivities and characteristic impedances versus thickness of vertical substrate ($\epsilon_{r1} = 4.5$, $t_1 = 0.8$ mm, $\epsilon_{r2} = 2.15$, $h = 3.5$ mm, $d = 0$).

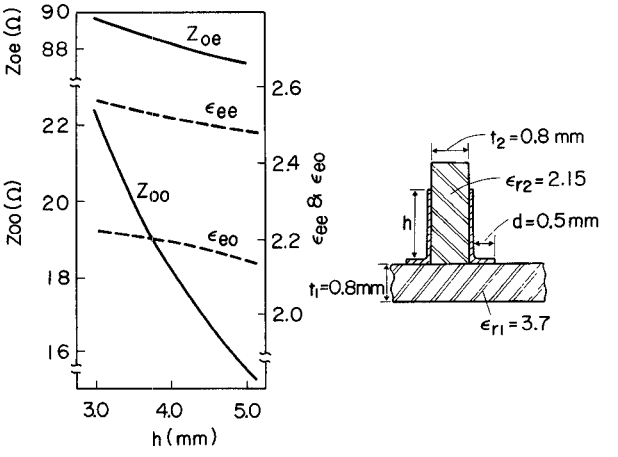

Fig. 9. Effective permittivities and characteristic impedances versus electrode height of vertical substrate in the case where $d \neq 0$.

If a supplemental electrode 5 is added on the main substrate beside the vertical electrodes (i.e., $d > 0$), not only does the characteristic impedance of the even mode decrease noticeably, but the effective permittivity of the even mode increases destructively. In order to keep almost the same value of the effective permittivity as that of the odd mode, it will be necessary to use a thicker material or a material of lower permittivity for the main substrate. Taking commonly available materials into consideration, we have calculated the dependence of the impedances on the electrode height of the VIP substrate. The result (Fig. 9) shows that the permittivity of the main substrate is still too large to obtain the required effective permittivity. But

it will be relieved by selecting a VIP substrate of higher permittivity.

In practice, the main substrate is often predetermined not only by its electrical characteristics but also by such other requirements as cost, availability, and size. Hence, it is most probable that one has to tune Z_{0o} by arranging the parameters of the vertical substrate on the given main substrate (given Z_{0e}). Therefore, selection of the vertical substrate will involve considerations of material thickness and electrode height.

III. Scattering Matrix of Coupled Lines with Structural Symmetry

The eigenvectors of a coupled line with twofold symmetry shown in Fig. 1 are known to be

$$u_1 = \begin{bmatrix} 1 \\ 1 \\ 1 \\ 1 \end{bmatrix} \quad u_2 = \begin{bmatrix} 1 \\ 1 \\ -1 \\ -1 \end{bmatrix}$$

$$u_3 = \begin{bmatrix} 1 \\ -1 \\ 1 \\ -1 \end{bmatrix} \quad u_4 = \begin{bmatrix} 1 \\ -1 \\ -1 \\ 1 \end{bmatrix}. \tag{5}$$

The corresponding eigenvalues are derived in the following way. Let the relation between voltages and currents at four ports be set as

$$v = \begin{bmatrix} v_1 \\ v_2 \\ v_3 \\ v_4 \end{bmatrix} = \begin{bmatrix} z_{11} & z_{12} & z_{13} & z_{14} \\ z_{21} & z_{22} & z_{23} & z_{24} \\ z_{31} & z_{32} & z_{33} & z_{34} \\ z_{41} & z_{42} & z_{43} & z_{44} \end{bmatrix} \begin{bmatrix} i_1 \\ i_2 \\ i_3 \\ i_4 \end{bmatrix} = [Z]i. \tag{6}$$

Suppose now that the current vector i equals the eigenvector u_1, or unit currents flow into all ports. In other words, two lines are excited symmetrically. The current at the center of the coupled line is zero in this even-mode excitation, the line being virtually open-circuited there. For this mode, the following relation holds:

$$z_1 = \frac{v_1}{i_1} = \frac{v_2}{i_2} = \frac{v_3}{i_3} = \frac{v_4}{i_4} = -jZ_{0e}\cot\frac{\theta_e}{2} \tag{7}$$

where Z_{0e} and θ_e are the characteristic impedance and phase angle for the even mode, respectively. The quantity z_1 is the eigenvalue for the eigenvector u_1.

In the same manner, we can find the remaining relations as

$$z_2 = jZ_{0e}\tan\frac{\theta_e}{2}$$

$$z_3 = -jZ_{0o}\cot\frac{\theta_o}{2}$$

$$z_4 = jZ_{0o}\tan\frac{\theta_o}{2} \tag{7'}$$

where Z_{0o} and θ_o are the characteristic impedance and phase angle for the odd mode, respectively.

From the general relation between the impedance matrix $[Z]$ and the scattering matrix $[S]$,

$$[S] = \{[Z]-[I]\}/\{[Z]+[I]\}$$

the eigenvalue of the $[S]$ matrix is written as

$$s_i = \frac{z_i - 1}{z_i + 1}. \tag{8}$$

We can find the S matrix of the symmetrical coupler as

$$[S] = \frac{1}{4}[u_1 \quad u_2 \quad u_3 \quad u_4]\cdot\operatorname{diag}[s_1 \quad s_2 \quad s_3 \quad s_4] \cdot[u_1 \quad u_2 \quad u_3 \quad u_4]^{-1}$$

$$= \frac{1}{4}\begin{bmatrix} 1 & 1 & 1 & 1 \\ 1 & 1 & -1 & -1 \\ 1 & -1 & 1 & -1 \\ 1 & -1 & -1 & 1 \end{bmatrix}\begin{bmatrix} s_1 & & & 0 \\ & s_2 & & \\ & & s_3 & \\ 0 & & & s_4 \end{bmatrix} \cdot\begin{bmatrix} 1 & 1 & 1 & 1 \\ 1 & 1 & -1 & -1 \\ 1 & -1 & 1 & -1 \\ 1 & -1 & -1 & 1 \end{bmatrix}^{-1}. \tag{9}$$

The above equation yields the characteristics of the coupler:

$$[S] = \begin{bmatrix} \gamma & \beta & \alpha & \delta \\ \beta & \gamma & \delta & \alpha \\ \alpha & \delta & \gamma & \beta \\ \delta & \alpha & \beta & \gamma \end{bmatrix} \tag{10}$$

where

$$\alpha = (s_1 - s_2 + s_3 - s_4)/4$$

$$\beta = (s_1 + s_2 - s_3 - s_4)/4$$

$$\gamma = (s_1 + s_2 + s_3 + s_4)/4$$

$$\delta = (s_1 - s_2 - s_3 + s_4)/4. \tag{11}$$

It will be convenient to prepare a chart for coupling, directivity, and input return loss versus Z_{0e} and Z_{0o}. It is possible to design a directional coupler with the desired characteristics using this chart, because Z_{0e} and Z_{0o} can be controlled almost independently in a VIP coupler, as is explained in the next section.

The coupling is defined to be the ratio $|\beta/\alpha|$, the directivity is $|\delta/\alpha|$ and the input return loss is $1/|\gamma|$.

Approximate values of α, β, γ, and δ are estimated using (7), (8), (10), and (11) with the assumption $\theta_e = \theta_o = \pi/2$:

$$\alpha = j\frac{(z_{0e}+z_{0o})(1+z_{0e}z_{0o})}{(1+z_{0e}^2)(1+z_{0o}^2)}$$

$$\beta = \frac{z_{0e}^2 - z_{0o}^2}{(1+z_{0e}^2)(1+z_{0o}^2)}$$

$$\gamma = \frac{z_{0e}^2 z_{0o}^2 - 1}{(1+z_{0e}^2)(1+z_{0o}^2)}$$

$$\delta = j\frac{(z_{0e}-z_{0o})(z_{0e}z_{0o}-1)}{(1+z_{0e}^2)(1+z_{0o}^2)} \tag{12}$$

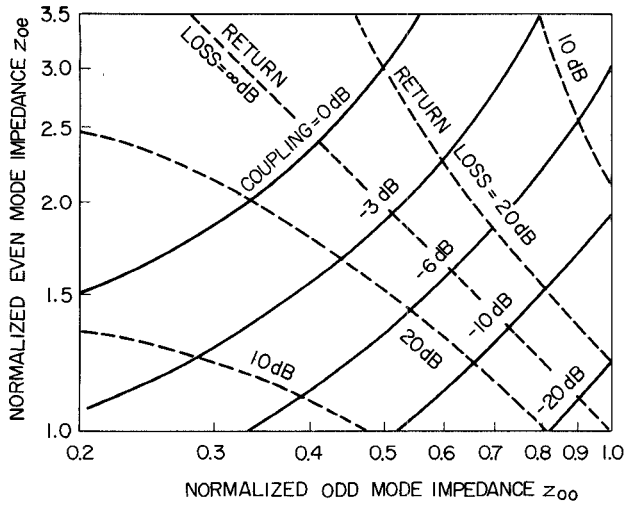

Fig. 10. Chart of coupling and return loss versus normalized even- and odd-mode impedances.

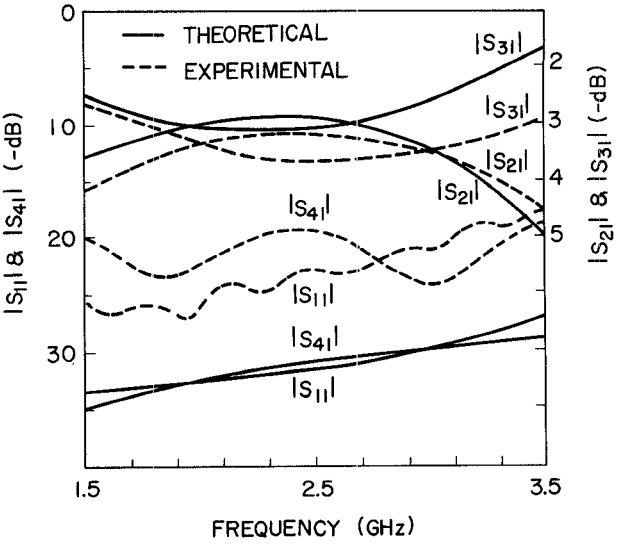

Fig. 11. Frequency characteristics of scattering matrix elements, theoretical and experimental ($\epsilon_{r1} = 4.5$, $t_1 = 0.8$ mm, $t_{r2} = 2.15$, $t_2 = 0.8$ mm, $h = 4.0$ mm, $d = 0$).

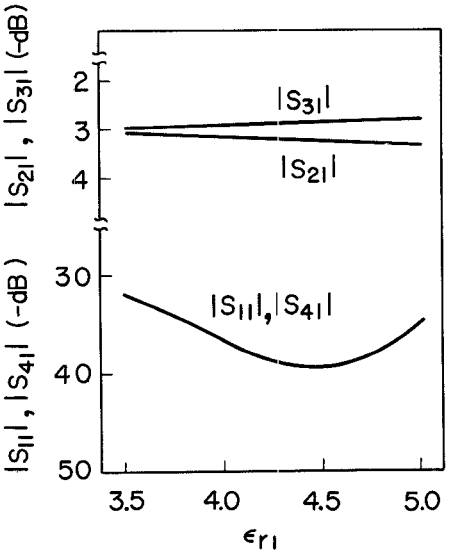

Fig. 12. Scattering matrix elements versus permittivity of main substrate ($t_1 = 0.8$ mm, $\epsilon_{r2} = 2.15$, $t_2 = 0.8$ mm, $h = 3.5$ mm, $d = 0$).

where z_{0e} and z_{0o} are even- and odd-mode impedances normalized to the characteristic impedance of the input or output line to be connected. The effective dielectric constants of both modes are assumed to be equal and the signal frequency is taken at the center of the band in (12).

Fig. 10 shows the values of coupling and return loss of the VIP circuit with respect to even- and odd-mode impedances. It shows that a directional coupler of satisfactory characteristics can be realized for wide range of z_{0e} and z_{0o} values. For example, a 3-dB coupler (coupling = 0 dB) has a return loss of more than 20 dB when z_{0o} is in the range of $0.34 \leqslant z_{0o} \leqslant 0.5$ and z_{0e} is adjusted according to Fig. 10.

In above calculation, we assumed $\theta_e = \theta_o$, although the discrepancy can be as much as 10 percent, as shown in Figs. 5–8, depending on the parameters of the VIP couplers. This discrepancy usually degrades the input return loss and isolation, and shifts the center frequency of optimum operation of the directional coupler. These effects will be examined in the next section.

IV. Characteristics of VIP Couplers

The frequency characteristics of the VIP coupler which is shown in Fig. 4 have been calculated and are shown in Fig. 11. Experimental results are also shown with broken curves. A test sample was made using a glass-epoxy substrate as the main board and a Teflon substrate as a vertical piece. The theoretical and the experimental curve of the coupling $|s_{21}|$ and the insertion loss in the through line $|s_{31}|$ agree well, although there is some dissipation loss and a small shift of the center frequency. The discrepancy between the theoretical and the experimental values in the return loss $|s_{11}|$ and the directivity $|s_{41}|$ is mainly caused by the residual return loss in the measurement system, which is above 25 dB.

The magnitude of scattering matrix elements $|s_{11}|$, $|s_{21}|$, $|s_{31}|$, and $|s_{41}|$ at the center frequency of the useful band were calculated and are shown in Figs. 12 through 15. It is seen in Figs. 12 and 13 that the coupling $|s_{21}|$ and the insertion loss in the through line $|s_{31}|$ do not change appreciably if the permittivity of the main or vertical substrate changes.

Fig. 14 shows the dependence of the matrix elements on the height of the vertical conductor. Both outputs $|s_{21}|$ and $|s_{31}|$ exchange their magnitudes according to the height h. Experimental results are also shown with broken curves in the figure. They agree well with theoretical curves.

In practice, as a vertical substrate, one can use a simple rectangular piece cut from a raw substrate material with conductors on both surfaces. This simplifies the production process of the VIP circuit because the etching process is omitted in the manufacture of the vertical piece. It also simplifies the adjustment of the height of the vertical conductors. We actually used this structure for the experiment in Fig. 14.

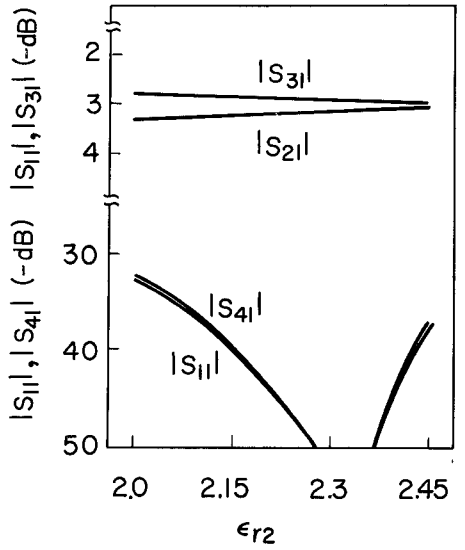

Fig. 13 Scattering matrix elements versus permittivity of vertical substrate ($\epsilon_{r1} = 4.5$, $t_1 = 0.8$ mm, $t_2 = 0.8$ mm, $h = 3.5$ mm, $d = 0$).

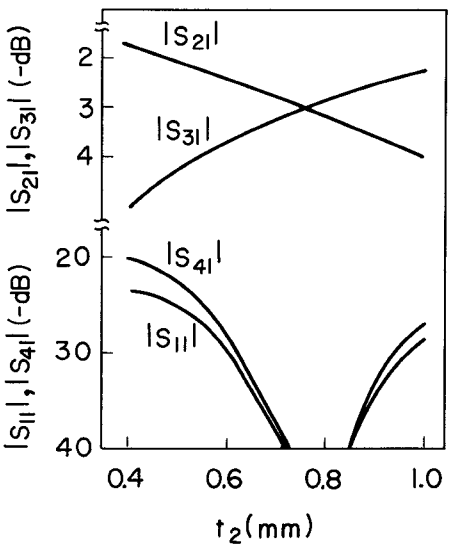

Fig. 15. Scattering matrix elements versus thickness of vertical substrate ($\epsilon_{r1} = 4.5$, $t_1 = 0.8$ mm, $\epsilon_{r2} = 2.15$, $h = 3.5$ mm, $d = 0$).

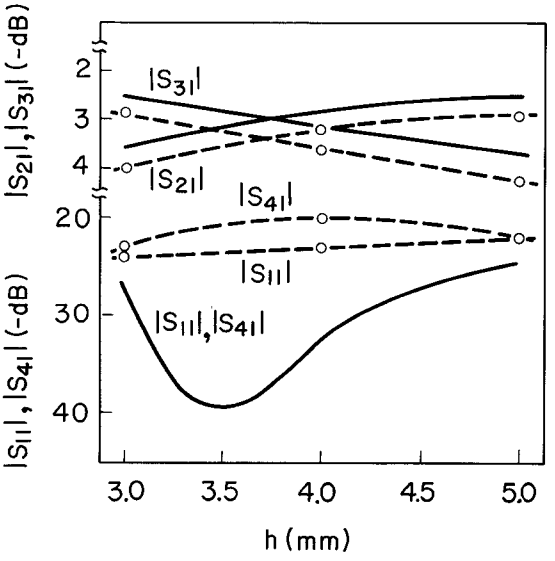

Fig. 14. Scattering matrix elements versus electrode height on vertical substrate, theoretical and experimental results ($\epsilon_{r1} = 4.5$, $t_1 = 0.8$ mm, $\epsilon_{r2} = 2.15$, $t_2 = 0.88$ mm, $d = 0$).

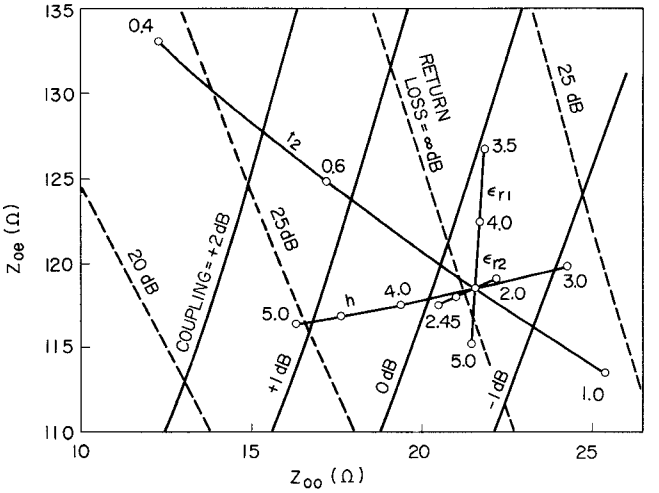

Fig. 16. Simplified chart of coupling and return loss versus even- and odd-mode impedances of VIP couplers (curves labeled ϵ_{r1}, ϵ_{r2}, h, and t_2 correspond to Figs. 5, 6, 7, and 8, respectively; h and t_2 are in unit of mm).

The thickness of the VIP substrate has a strong influence on the coupling, as is shown in Fig. 15. Since various substrate thicknesses are available commercially, the coupling ratio can be easily adjusted.

Even if effective permittivities for the even and odd modes are somewhat different from each other, serious degradation in the isolation or input return loss is not observed in Figs. 12–15.

Finally, in order to give a design idea of the VIP directional coupler, the previous results are summarized and shown in Fig. 16. Since a 3-dB coupler is our main concern, only the area of interest of Fig. 10 is shown in the figure. The source and load impedances are taken as 50 Ω. Several lines are drawn in the figure, which show the even- and odd-mode impedances for given values of parameters.

For example, the height of the electrodes on the vertical substrate is varied from 3.0 to 5.0 mm along the curve marked h, keeping the other parameters the same as in Fig. 4. In this way, from Fig. 16, one can find coupling and return loss for given value of h, which are very close to the accurate values computed in Fig. 14. This is true for other curves; therefore, Fig. 16 is useful for the practical design of the VIP directional couplers.

From Fig. 16, it is also noticed that alteration of the permittivity ϵ_{r2} of the vertical substrate changes the odd-mode impedance while the even-mode impedance remains almost unchanged. On the other hand, alteration of the permittivity ϵ_{r1} of the main substrate has a contrary effect. The tilted line with the thickness t_2 of the VIP substrate is roughly perpendicular to the constant coupling curves. This means that changing the thickness of the VIP sub-

strate is most effective when adjusting the coupling ratio of the VIP circuit.

V. Conclusions

A directional coupler of VIP structure has been analyzed making use of the boundary element method. Effective permittivities and characteristic impedances for both even and odd modes were obtained numerically and they were substituted into the scattering matrix formula to obtain the parameters for a symmetrical directional coupler. The agreement of theoretical and experimental results was satisfactory.

Furthermore, a simplified design chart has been drawn, which is useful because Z_{0e} and Z_{0o} are controllable almost independently by varying the main and VIP substrates, respectively.

A VIP 3-dB coupler is especially suited for *L*- or *S*-band applications because of its small size and low cost.

References

[1] K. C. Gupta *et al., Microstrip Lines and Slotlines.* Norwell, MA: Artech House, 1979, pp. 303–361.
[2] W. J. Getsinger, "A coupled strip-line configuration using printed-circuit construction that allows very close coupling," *IRE Trans. Microwave Theory Tech.*, vol. MTT-9, pp. 535–544, Nov. 1961.
[3] S. B. Cohn, "Characteristic impedances of broadside-coupled strip transmission lines," *IRE Trans. Microwave Theory Tech.*, vol. MTT-8, pp. 633–637, Nov. 1960.
[4] Y. Konishi, I. Awai, and Y. Fukuoka, "Newly proposed vertically installed planar circuit and its application," *IEEE Trans. Broadcast.*, vol. BC-33, pp. 1–7, Mar. 1987.
[5] C. A. Brebbia, *Progress in Boundary Element Methods*, vol. 1, Pentech Press, 1982.

Yoshihiro Konishi (A'61–SM'65–F'81) was born on September 24, 1928, in Nara, Japan. He received the bachelor of engineering and doctor of engineering degrees from Kyoto University, Japan, in 1951 and 1961, respectively.

He joined Nippon Hoso Kyokai (NHK, Japan Broadcasting Corporation) in 1951. From 1962 to 1963, he was a visiting scholar at the Microwave Research Institute of the Polytechnic Institute of Brooklyn, NY. From 1976 to 1978, he was a project manager of a joint experiment carried out by NHK and NASA on a satellite earth station. He joined the Uniden Corporation in November 1983, where he is now a senior executive vice president.

Dr. Konishi received the Medal with Purple Ribbon from the Japanese Emperor in 1982. In addition, he received awards from the Ministry of Posts in 1978, the Patent Bureau in 1977, and the Ministry of Science and Technology in 1979. He is senior editor for Asia of the Broadcast Technology Society and has served on the editorial board of the Transactions on Microwave Theory and Techniques.

Ikuo Awai (M'78) was born in Bujun, Japan, on February 28, 1941. He received the B.S. degree in 1963, the M.S. degree in 1965, and the Ph.D. degree in 1978, all from Kyoto University, Kyoto, Japan.

In 1967, he joined the Department of Electronics, Kyoto University, as a Research Associate, where he was engaged in research on microwave magnetic waves and integrated optics. He is now an engineering director at the Uniden Corporation. His current research interests include microwave amplifiers and oscillators.

Dr. Awai is a member of the Institute of Electronics and Communication Engineers of Japan.

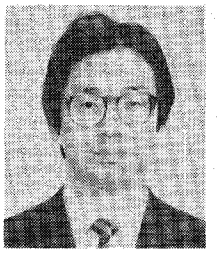

Yoshiro Fukuoka (S'81–M'84) was born in Osaka, Japan, in October 1956. He received the B.S. and M.S. degrees from the University of Electro-Communications in 1979 and 1981, respectively, and the Ph.D. degree from the University of Texas at Austin in 1984.

He then joined Uniden Satellite Technology in August 1984, where he mainly worked on TVRO systems. He is currently an engineering manager at the Uniden Corporation. His current research interests are in printed circuit components and microwave and millimeter-wave integrated circuits.

Dr. Fukuoka is a member of the Institute of Electronics and Communication Engineers of Japan.

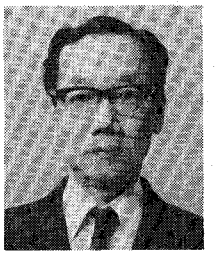

Masamitsu Nakajima (S'65–M'66) graduated from Kyoto University, Japan, in 1960. He received the Ph.D. degree from Kyoto University in 1967.

In 1965 he joined the Electronics Department of Kyoto University, where he is now an Associate Professor. His research has involved parametric amplifiers, solid-state microwave oscillators and amplifiers, synchronization of oscillators and power combination, high-power millimeter waves for nuclear fusion plasma, guided-wave optics, and light modulators for optical communication.

Dr. Nakajima is the author of the books *Microwave Engineering—Foundations and Principles* and *Fundamental Electronic Circuits* (in Japanese).